Spin filtering and spin separation in 2D materials by topological spin Hall effect

Andrei Zadorozhnyi and Yuri Dahnovsky

Department of Physics and Astronomy/3905

1000 E. University Avenue

University of Wyoming

Laramie, WY 82071

(Dated: March 1, 2021)

Abstract

The needs of high speed performance electronic devices for various applications require novel materials and new physical phenomena. For these purposes we propose to study new physical effects based on electron scattering on magnetic skyrmions and vortices distributed in a 2D ferromagnetic material. We show that the topological spin Hall effect (TSHE) can be efficiently employed for the filtering, switching, and separation of spin currents. For some values of the parameters (conduction electron concentrations, and skyrmion/vortex sizes) it is possible to separate Hall currents for different electron spin projections as it is like for different carrier charges (electrons and holes) in the normal Hall effect. The calculations are performed using the Boltzmann kinetic equation for the nonequilibrium distribution function and the Lippmann-Schwinger equation for the transition matrix in the whole range of the adiabaticity parameter. The spin filtering due to the skyrmion/vortex scattering can be several orders of magnitude more efficient in the narrow range of the electron concentrations than that of the ordinary ferromagnetic spin polarization in spintronics.

The nature of topological spin Hall effect (TSHE) is different than a charge Hall effect where a charge is deviated from its straight line trajectory due to the Lorentz force in an external magnetic field. A TSHE appears due to the interaction of conducting electrons (holes) with the localized magnetic moment textures – skyrmions,[1–14] which are due to spin-orbit interaction, i.e., specifically Dzyaloshinski-Moriya interaction term.[1,10]

There are several approaches to calculate TSHE for weak conducting electron-skyrmion interaction. A topological spin current can be found[15,16] For adiabatic electron-skyrmion scattering, the tight-binding approximation[17,18] and the Berry phase approach[14,19] were also employed. However, the semiclassical approach based on the nonequilibrium Boltzmann equation[1,20–30] allows us to find spin currents in the whole range of the adiabaticity parameter. In this approach the main problem is in the calculation of a collision integral, which is due to the conduction electron scattering at the localized magnetic moment texture.

For applications it is important to understand how partial spin current densities depend on various parameters such as an electron density, a magnetic moment of the ferromagnet, Fermi energy, an exchange integral for localized and conduction electron spins. The effect of electron scattering at skyrmions and vortices can have a tremendous impact on the development of novel spintronic devices. In this research we demonstrate that the current density strongly depends on a spin orientation and other parameters of the system. We show that the currents can be separated according their spin projection (*separation*). At some values of the parameters electric current with spin-down can be substantially suppressed (*filtration*). We demonstrate that, despite spin polarization can also take place in an ordinary ferromagnet, the presence of skyrmions can additionally enhance the polarization by several orders of magnitude. Thus, in this work we are interested in partial spin-oriented currents driven by the TSHE. In particular, we consider a free electron particle moving in a 2D crystal where a spin texture is introduced by localized magnetic moments (skyrmions and vortices) at low concentrations where each scattering is independent of other scattering processes. The schematic picture of the spin Hall electron scattering is shown in Fig. 1. To describe the topological spin Hall scattering we employ the *s*-*d* Hamiltonian where the interaction between the localized moments and spins of the conduction electrons is chosen in the exchange form:[31]

$$H = \frac{k^2}{2m} - J\mathbf{S}(\mathbf{r}) \cdot \boldsymbol{\sigma}, \tag{1}$$

where the first term represents the kinetic energy of conduction electrons, J is an exchange

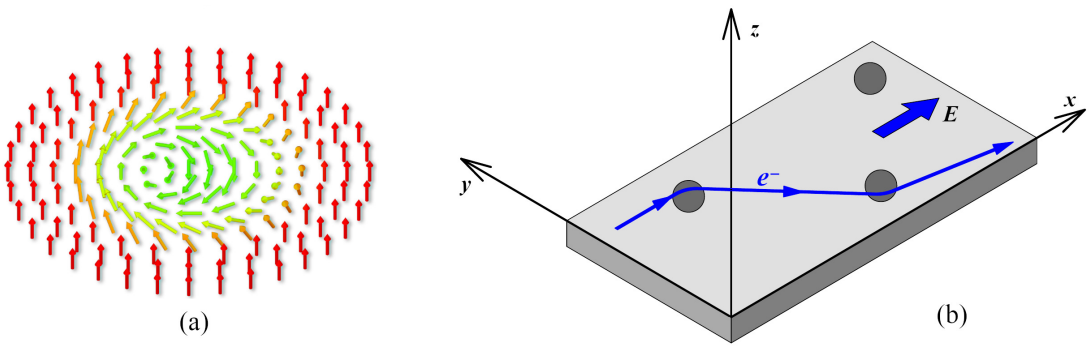

FIG. 1: (a) Skyrmion and (b) the system of the magnetic skyrmions randomly distributed in a 2D material where the electron current is due to an external electric field.

integral, $\mathbf{S(r)}$ is a localized magnetic moment (in this work we only consider skyrmions and vortices), and $\boldsymbol{\sigma}$ is a vector with the three Pauli matrix projections for the conduction electron spins. We choose the $\mathbf{S(r)}$ texture in the following form:

$$\mathbf{S}(\mathbf{r}) = S_0 \cdot \mathbf{e}_z + \sum_i \delta\mathbf{S}(\mathbf{r} - \mathbf{r_i}), \tag{2}$$

where S_0 is uniform out-of-plane background magnetization and $\delta\mathbf{S}(\mathbf{r} - \mathbf{r_i})$ is a deviation of magnetic moment due to the skyrmion or vortex. The conduction electrons are a uniform electron gas embedded into the ferromagnetic and skyrmion environment. Because of the splitting of the energy for different spin projections, we can introduce two types of carriers depending on a spin orientation. For spin $\uparrow$ and spin $\downarrow$ we write the following kinetic energies $\varepsilon^{\uparrow,\downarrow}(\mathbf{k}) = k^2/(2m) \pm J/2$. For the two types of electrons we can define momenta in the following way:

$$k^{\uparrow,\downarrow} = \frac{\sqrt{2m(\varepsilon \pm J/2)}}{\hbar}. \tag{3}$$

To determine electron current density in x- and y-directions we have to find a nonequilibrium distribution function described by the Boltzmann equation in the stationary state,[32] where the transition probability, $W^{ss'}_{\mathbf{pp'}}$, can be determined in terms of a transition matrix $T^{ss'}_{\mathbf{pp'}}$:

$$W^{ss'}_{\mathbf{pp'}} = \frac{2\pi}{\hbar} n_t \left| T^{ss'}_{\mathbf{pp'}} \right|^2 \delta(\varepsilon - \varepsilon'), \tag{4}$$

where s, s' are free electron spin projections. The transition matrix can be found from the Lippmann-Schwinger equation equation:[33]

$$\hat{T} = \hat{V} + \hat{V}\hat{G}_0\hat{T}, \tag{5}$$

where $\hat{G}_0$ is a retarded free electron Green's function.[34] The potential energy for a single spin texture is given by the following matrix:

$$\hat{V}(\mathbf{r}) = -JS_0 \begin{pmatrix} n_z - 1 & n_x - in_y \\ n_x + in_y & -n_z + 1 \end{pmatrix}. \tag{6}$$

Here $n_x^2 + n_y^2 + n_z^2 = 1$. Furthermore, we assume that the skyrmion amplitude is the same as that of the background magnetization. We solve the Boltzmann equation for a non-equilibrium distribution function, which is presented as $f^s(\mathbf{k}) = f_0(\mathbf{k}) + f_1^s(\mathbf{k})$. Here f_0 is the Fermi equilibrium distribution function and the non-equilibrium part, f_1^s, is expressed in the following way:[32]

$$f_1^s(\mathbf{k}) = -\frac{\partial f_0}{\partial \varepsilon} \boldsymbol{\chi}^s(\varepsilon) \cdot \mathbf{k}, \tag{7}$$

where $\boldsymbol{\chi}^s$ is an unknown vector function depending on the electron energy. The Boltzmann equation for $\boldsymbol{\chi}^s$ is a 4×4 algebraic matrix equation that can be easily solved if the matrix elements are known. To determine these matrix elements we have to find the solution of the Lippmann-Schwinger equation (5) and then determine the transition probability (4).

Eq. (5) is a 4×4 integral equation that can be numerically solved the $\mathbf{k}$-representation. The 2D-free electron wave functions are used as a basis set. For spin textures such as skyrmions and vortices, there is a polar symmetry in a 2D k-space. Indeed, polar symmetry takes place where the transfer matrix elements $T^{ss'}_{\mathbf{kk}'}$ are independent of the incident and scattering angles separately and depend only on the angle between $\mathbf{k}$ and $\mathbf{k}'$ wave vectors. This feature substantially simplifies the calculations. By applying the Fourier transform, the radial symmetry allows us to present the T-matrix in a block-diagonal form. Within the conditions mentioned above we have found the solution for T-matrix for any strength of the scattering potential, i. e., in the whole range of the adiabaticity parameter.[30]

As soon as a nonequilibrium function is determined (see Eq. (7)) at zero-temperature, the energy derivative over the Fermi distribution becomes the delta function, and then the 2D electric current densities in x- and y-directions becomes:[32]

$$j^s_{x,y} = e \int v_{x,y} f_1^s(\mathbf{k}) dk_x dk_y = \frac{e}{4\pi\hbar} k_F^s \chi^s_{x,y}. \tag{8}$$

From this equation we conclude that only electrons with $k^\uparrow = k_F^\uparrow$ and $k^\downarrow = k_F^\downarrow$ contribute to the current. $k_F^\uparrow$ and $k_F^\downarrow$ are defined by Eq. (3).

In this research we are interested in the spin-↑ and spin-↓ current densities depending on the following dimensionless parameters:

$$\varkappa a = \frac{\sqrt{2mJ}}{\hbar} a, \qquad \Gamma = \frac{2\varepsilon_F}{J}. \tag{9}$$

The first parameter, $\varkappa a$, describes a dimensionless skyrmion (vortex) size. The second parameter, Γ, defines dimensionless Fermi energy that is proportional to the electron density of a 2D free electron gas. As far as skyrmion and vortex analytic formulas are concerned, we choose the following forms describing Bloch skyrmion[35] and vortex shapes, respectively:

$$\begin{aligned} n_z(r) &= \cos\left[\pi\left(1-\exp\left(-\frac{r^2}{a^2}\right)\right)\right], \\ n_z(r) &= \cos\left[\pi\left(\exp\left(-\frac{r^2}{a^2}\right)-\exp\left(-\frac{(c_1 r)^2}{a^2}\right)\right)c_2\right]. \end{aligned} \tag{10}$$

The first equation corresponds to a skyrmion and the second one describes a vortex, where the coefficients c_1 and c_2 allow us to change the minimum location and normalize the spin distribution function. For the calculations we choose $c_1 = 3.2$, that places minimum approximately at $r = 0.5a$, and $c_2 \simeq 1.4255$. For both skyrmion and vortex, the x- and y-components of the spin textures are determined as $n_x = \cos(\varphi)\sqrt{1-n_z^2}$ and $n_y = -\sin(\varphi)\sqrt{1-n_z^2}$, respectively. Here φ is a polar angle.

For the calculations we choose skyrmions with the topological charge $Q = 1$ and vortices with the topological charge $Q = 0$. In Fig.2 a and b for both skyrmions and vortices we present conductivities $\alpha_{xx}^{\uparrow,\downarrow}$ (see Fig.2a), and $\alpha_{xy}^{\uparrow,\downarrow}$ (see Fig.2b), respectively.

In Fig. 2a $\varkappa a = 0.05$, i.e., the size of the skyrmion is very small, and the spin-up electric conductivity in the x-direction for both skyrmions and vortices is large and represented by straight lines. For spin-down the conductivity vanishes at $\Gamma = 1$ according to Eq. (3). As far as xy-conductivity is concerned (the Hall conductivity), it is the five orders of magnitude smaller than the xx-conductivity as shown in Fig. 2b. The spin Hall conductivity demonstrates nonlinear monotonic growth for both skyrmions and vortices and also spin-up and spin-down projections. However, the skyrmion-induced spin Hall conductivity is larger than the vortex one. For all dependencies the spin-down conductivity is always larger than the spin-up one. For small value of Γ the ratio of spin-up to spin-down xy-conductivity can be very large. Thus, we observe a *filtering* effect for small Γs.

For the intermediate values of skyrmion and vortex sizes, $\varkappa a = 1.0$, the dependencies are nonlinear and more dramatic. Indeed, for α_{xx} the skyrmion spin-up conductivity decreases

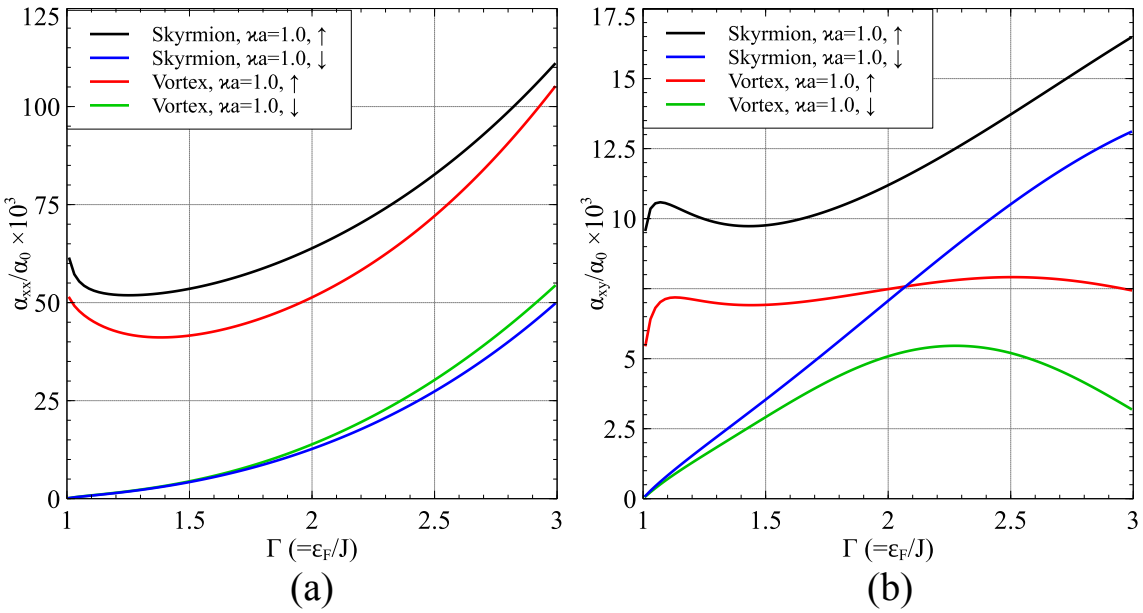

FIG. 2: (a) $\alpha_{xx}^{\uparrow,\downarrow}$ for both skyrmion and vortex (b) $\alpha_{xy}^{\uparrow,\downarrow}$ for both skyrmion and vortex for small skyrmion and vortex size with $\varkappa a = 0.05$. Here α_0 is a normalization electroconductivity, the same for all calculations,

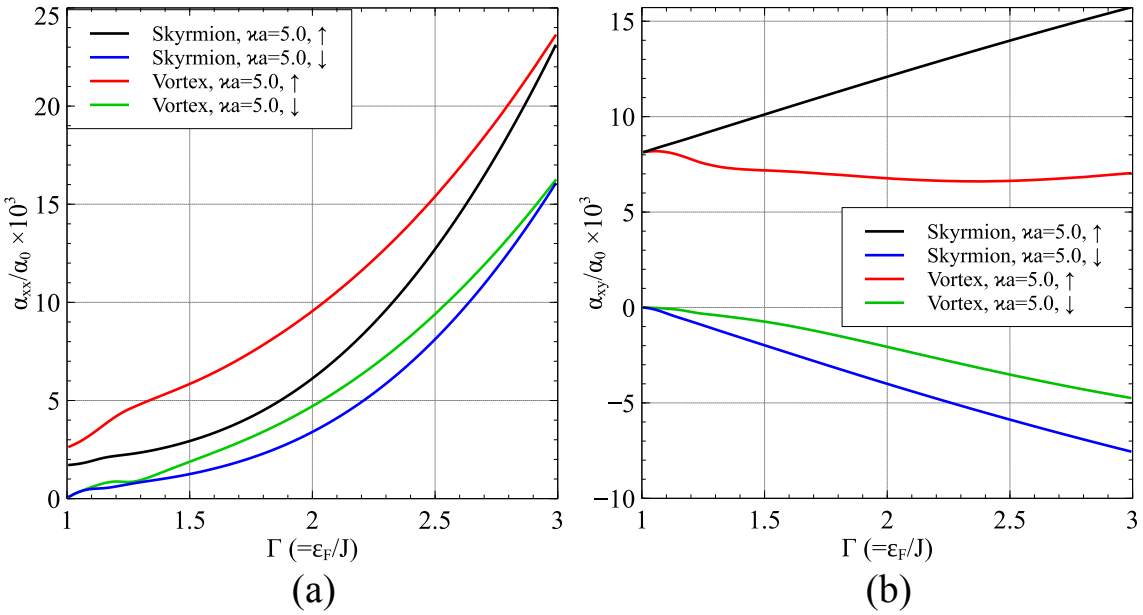

FIG. 3: (a) $\alpha_{xx}^{\uparrow,\downarrow}$ for both skyrmion and vortex (b) $\alpha_{xy}^{\uparrow,\downarrow}$ for both skyrmion and vortex for intermediate skyrmion and vortex size with $\varkappa a = 1.0$.

in the broad range of Γ and then slowly increases. The vortex spin-up conductivity exhibits the minimum at $\Gamma \simeq 1.4$ and then goes up. The spin-down conductivities are nonlinear but monotonic and, as shown in Fig. 3a, it is larger for the vortex than for the skyrmion. The Hall conductivity is only about one order of magnitude smaller than α_{xx}. The spin-up Hall conductivity dependencies on the Γ parameter (electron concentration) exhibit the maxima at $\Gamma = 1.1 - 1.2$ for both skyrmion and vortex scattering. The spin-down Hall conductivity for the vortex demonstrates the maximum. This picture is entirely different than that of the small skyrmion sizes (see Fig. 2b). Such dependencies are nonlinear and difficult to predict.

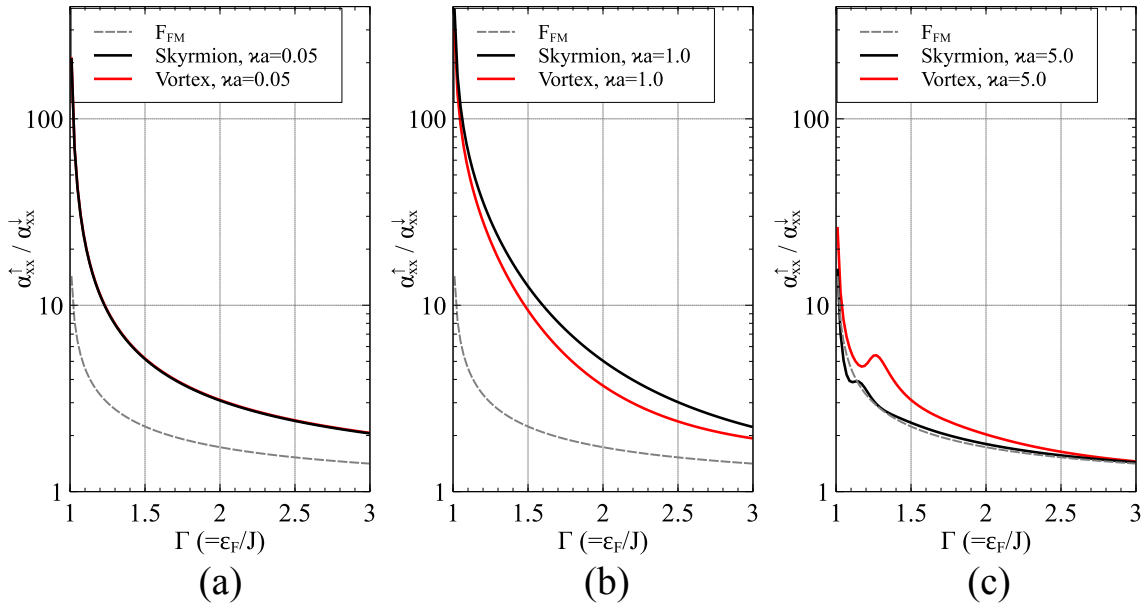

FIG. 4: (a) $\alpha_{xx}^{\uparrow,\downarrow}$ for both skyrmion and vortex (b) $\alpha_{xy}^{\uparrow,\downarrow}$ for both skyrmion and vortex for large skyrmion and vortex size with $\varkappa a = 5.0$.

For the large skyrmion size ($\varkappa a = 5.0$), the electron scattering is adiabatic and large. The skyrmion and vortex spin-dependent α_{xx} and α_{xy} are of the same order of magnitude. As shown in Fig. 4a, α_{xx} are monotonically growing functions for both skyrmion and vortex and for spin-up and spin-down electrons. In this case the spin-down conductivity is of the same order of magnitude as the spin-up one. For the spin Hall effect (Fig. 4b) we observe the separation of currents for spin-up and spin-down states. Interestingly, the spin-up and spin-down conductivities for a vortex are monotonically decreasing and almost parallel functions of Γ. In the skyrmion case, the dependence is significantly different. The spin-up spin Hall conductivity $\alpha_{xy}^{\uparrow}$ is a linearly growing function while $\alpha_{xy}^{\downarrow}$ is linearly

decreasing function. For both skyrmion and vortex, spin-down current is negative while spin-up is always positive. Thus, we observe the *separation* of spin current (left and right) that can be used in applications.

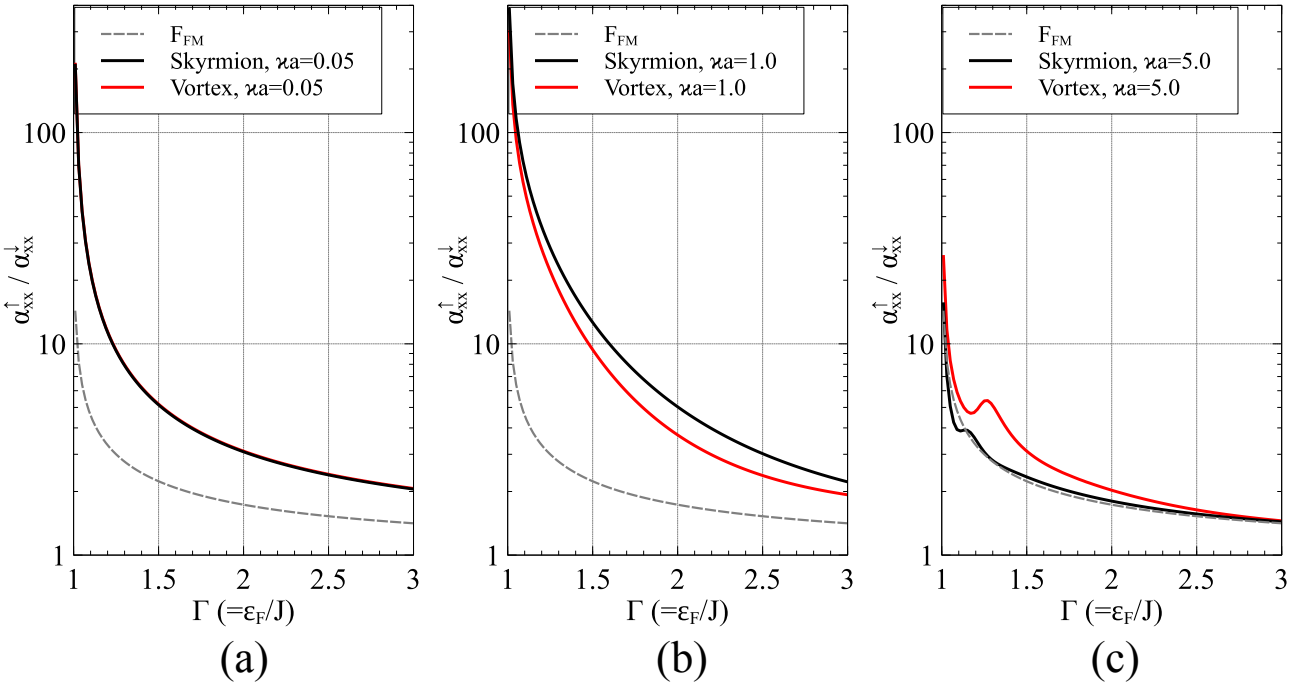

FIG. 5: Filtration coefficient, F, for the skyrmion/vortex sizes: (a) $\varkappa a = 0.05$ (b) $\varkappa a = 1.0$, and (c) $\varkappa a = 5.0$. The grey dashed line represents the ferromagnetic filtering coefficient, F_{FM}.

Despite of the topological spin texture like a skyrmion and vortex, there is spin *filtering* due to the existence of the background ferromagnetic ordering. In this case, it is important to understand, which effect contributes at most: the ferromagnetic polarization or filtering due to skyrmion scattering. The filtering effect will be calculated as a filtration coefficient defined as follows:

$$F \equiv \frac{\alpha_{xx}^{\uparrow}}{\alpha_{xx}^{\downarrow}}. \tag{11}$$

For the ferromagnetic filtering, $\alpha_{xx}^{\uparrow} \sim k_F^{\uparrow}$ and $\alpha_{xx}^{\downarrow} \sim k_F^{\downarrow}$, so, using Eqs. 3 the ratio equals $F_{FM} = \sqrt{(\Gamma+1)/(\Gamma-1)}$. F can be also calculated for the skyrmion and vortex spin textures. We compare these two cases for different values of $\varkappa a$ (0.05, 1.0, 5.0) as a function of Γ. The results are presented in Fig. 5 a, b, and c.

As shown in Fig. 5a, the skyrmion/vortex curves are close to the F_{FM} one at the intermediate and large Γs, while there is a significant difference, about one order of magnitude,

at small values of Γs. At larger Γs, the filtration coefficient difference between F_{FM} and $F_{SK/VOR}$ is lower, but noticeable.

For the intermediate skyrmion/vortex sizes ($\varkappa a = 1.0$) we find that the filtering coefficient for the skyrmion is higher than that of the vortex as shown in Fig. 5b. At small Γs the ratio $F_{SK/VOR}/F_{FM}$ is greater than one order of magnitude, indicating that the filtering is mostly due to skyrmion/vortex rather than the ferromagnetic polarization.

For the large skyrmion (vortex) sizes ($\varkappa a = 5.0$), the situation is significantly different. In contrast to the intermediate skyrmion size (Fig. 5b), the filtering in more efficient for vortices rather than skyrmions. Moreover, we observe the nonmonotonic behavior, i.e., the peak at $\Gamma = 1.2$ for the skyrmion and $\Gamma = 1.3$ for the vortex. In the case of the skyrmion the filtration coefficient is almost the same as that of F_{FM}. Thus, for this case, the filtration is mostly determined by the ferromagnetic background.

For estimations we take the following parameters in Fe(4)/Co(4) multilayer film: $a = 10\ nm$, $m = 0.1m_e$, $J = 0.1\ eV$, and $\varepsilon_F = 0.3\ eV$.[36] In this case $\Gamma = 3$ and $\varkappa a = 5$. According to Fig. 4b the relative skyrmion spin separation Hall current is very large, $(\alpha^{\uparrow}_{xy} - \alpha^{\downarrow}_{xy})/(\alpha^{\uparrow}_{xx} + \alpha^{\downarrow}_{xx}) = 0.6$. For the small skyrmion with $\varkappa a = 0.05$ (see Fig. 2b) the relative spin Hall conductivity is extremely small, $(\alpha^{\uparrow}_{xy} - \alpha^{\downarrow}_{xy})/(\alpha^{\uparrow}_{xx} + \alpha^{\downarrow}_{xx}) = 6.8 \cdot 10^{-6}$. Thus, the relative spin Hall splitting is significantly increased by five orders of magnitude due to the skyrmion electron scattering.

In *conclusion*, we have studied the behavior of electric currents is x- and y- (Hall effect) directions depending on the skyrmion/vortex sizes and carrier concentrations. We have found the strong *filtering* and spin *separation* for specific values of the parameters. For small skyrmion sizes the filtering can reach one order of magnitude in the x-direction. At small values of Γ the filtering in x- and y-directions can be many orders of magnitude. The filtering effect is due to both skyrmions scattering and ferromagnetic spin polarization. As shown in Fig. 5a, the filtering can be as much as ten times more efficient than that of the ferromagnetic background polarization. For the intermediate values of skyrmion sizes, we find the nonmonotonic behavior in α_{xx} and α_{xy} for skyrmions and vortices. At small values of Γ, the spin-up spin Hall current exhibits a sharp peak in the narrow range of Γs (carrier concentrations) that can be used as a *switch*. For the intermediate skyrmion sizes, the filtration is even more efficient than that of the small sizes. For large values of skyrmion size we have found the strong *separation* in spin Hall currents for both skyrmions and vortices.

For skyrmions, the separation is even more efficient.

Filtering and *separation* in topological Hall effect can be employed in spin electronic devices and as efficient elements in computers.

Acknowledgments

This work was supported by a grant from the U S National Science Foundation (No. DMR-1710512) and the U S Department of Energy (No. 1004389) to the University of Wyoming.

---

[1] Nagaosa N, Sinova J, Onoda S, MacDonald A H and Ong N P 2010 *Rev. Mod. Phys.* **82**(2) 1539–1592

[2] Lee M, Kang W, Onose Y, Tokura Y and Ong N P 2009 *Phys. Rev. Lett.* **102**(18) 186601

[3] Neubauer A, Pfleiderer C, Binz B, Rosch A, Ritz R, Niklowitz P G and Böni P 2009 *Phys. Rev. Lett.* **102**(18) 186602

[4] Machida Y, Nakatsuji S, Maeno Y, Tayama T, Sakakibara T and Onoda S 2007 *Phys. Rev. Lett.* **98**(5) 057203

[5] Sürgers C, Fischer G, Winkel P and Löhneysen H V 2014 *Nat. Commun* **5** 3400

[6] Ueland B *et al.* 2012 *Nat. Commun* **3**

[7] Fabris F W, Pureur P, Schaf J, Vieira V N and Campbell I A 2006 *Phys. Rev. B* **74**(21) 214201

[8] Ohuchi Y, Kozuka Y, Uchida M, Ueno K, Tsukazaki A and Kawasaki M 2015 *Phys. Rev. B* **91**(24) 245115

[9] Oveshnikov L N, Kulbachinskii V A, Davydov A B, Aronzon B A, Rozhansky I V, Averkiev N S, Kugel K I and Tripathi V 2015 *Sci. Rep* **5** 17158–17158

[10] Nagaosa N and Tokura Y 2013 *Nat. Nanotechnol* **8** 899–911

[11] Kanazawa N, Kubota M, Tsukazaki A, Kozuka Y, Takahashi K S, Kawasaki M, Ichikawa M, Kagawa F and Tokura Y 2015 *Phys. Rev. B* **91**(4) 041122

[12] Muhlbauer S, Binz B, Jonietz F, Pfleiderer C, Rosch A, Neubauer A, Georgii R and Boni P 2009 *Science* **323** 915–919

[13] Li Y, Kanazawa N, Yu X Z, Tsukazaki A, Kawasaki M, Ichikawa M, Jin X F, Kagawa F and Tokura Y 2013 *Phys. Rev. Lett.* **110**(11) 117202

[14] Bruno P, Dugaev V K and Taillefumier M 2004 *Phys. Rev. Lett.* **93**(9) 096806

[15] Onoda M, Tatara G and Nagaosa N 2004 *J. Phys. Soc. Jpn* **73** 2624–2627

[16] Tatara G and Kawamura H 2002 *J. Phys. Soc. Jpn* **71**

[17] Ohe J, Ohtsuki T and Kramer B 2007 *Phys. Rev. B* **75**

[18] Ndiaye P B, Akosa C A and Manchon A 2017 *Phys. Rev. B* **95**

[19] Ye J *et al.* 1999 *Phys. Rev. Lett.* **83** 3737–3740

[20] Luttinger J M and Kohn W 1955 *Phys. Rev.* **97**(4) 869–883

[21] Luttinger J M 1958 *Phys. Rev.* **112**(3) 739–751

[22] Smit J 1955 *Physica* **21** 877–887

[23] Berger L 1970 *Phys. Rev. B* **2**(11) 4559–4566

[24] Jungwirth T, Niu Q and MacDonald A H 2002 *Phys. Rev. Lett.* **88**(20) 207208

[25] Sinitsyn N A 2007 *J. Phys. Condens. Matter* **20** 023201

[26] Sinitsyn N A, MacDonald A H, Jungwirth T, Dugaev V K and Sinova J 2007 *Phys. Rev. B* **75**(4) 045315

[27] Sinitsyn N A, Niu Q and MacDonald A H 2006 *Phys. Rev. B* **73**(7) 075318

[28] Sinitsyn N A, Niu Q, Sinova J and Nomura K 2005 *Phys. Rev. B* **72**(4) 045346

[29] Denisov K S, Rozhansky I V, Averkiev N S and Lähderanta E 2016 *Phys. Rev. Lett.* **117**(2) 027202

[30] Denisov K S, Rozhansky I V, Averkiev N S and Lähderanta E 2018 *Phys. Rev. B* **98**(19) 195439

[31] Hewson A C 1993 *The Kondo Problem to Heavy Fermions* Cambridge Studies in Magnetism (Cambridge University Press)

[32] Anselm A 1981 *Introduction to Semiconductor Theory* (Mir, Moscow)

[33] Taylor J R 1972 *Scattering Theory: The quantum Theory on Nonrelativistic Collisions* (Wiley, New York)

[34] Fetter A L and Walecka J D 2003 *Quantum Theory of Many-Particle Systems* (Dover Publications, New York) ISBN 0486428273

[35] Pershoguba S S, Nakosai S and Balatsky A V 2016 *Phys. Rev. B* **94**(6) 064513

[36] Soumyanarayanan A, Raju M, Gonzalez Oyarce A L, Tan A K C, Im M Y, Petrović A P, Ho P, Khoo K H, Tran M, Gan C K, Ernult F and Panagopoulos C 2017 *Nature Materials* **16** 898–904